A coarse-grained tight binding method for electrostatic analysis of nanoelectromechanical systems (NEMS)

Y. Xu, G. Li and N.R.Aluru*

University of Illinois at Urbana-Champaign, Urbana, IL 61801
*aluru@uiuc.edu

ABSTRACT

A coarse-grained tight binding (CG-TBA) approach is presented for electrostatic analysis of NEMS. The key idea is to represent the entire NEM structure with a minimal number of unit cells but to accurately compute the electronic properties. The approach significantly reduces the computational cost but maintains the accuracy of the full TBA analysis.

Keywords: tight binding, nanoelectromechanical systems (NEMS), coarse-grained method

1 INTRODUCTION

Silicon electrostatic nanoelectromechanical systems (NEMS) [1] are one of the emerging applications in nanotechnology. As the critical length of a NEM structure shrinks to less than 30 nanometers, classical models based on continuum approximations become inaccurate in predicating the electronic properties of NEM structures. Tight binding approximations (TBA)[2]–[5] are typically more accurate in such cases. However, the computational cost involved in solving a TB system constructed using 3D crystal lattice structures (or unit cells) is very high even for small systems. In many NEMS applications, the electronic properties (e.g. the charge density) do not vary in some directions or over a large distance along a particular direction. The application of the classical TB method to model such NEMS applications requires that all the unit cells in all the three directions be taken into account. For typical NEMS examples, this can mean the use of hundreds of thousands of unit cells, which can be practically impossible to model with the classical TB method. If the number of unit cells can be reduced by using the fact that the electronic properties do not vary over a certain direction or over a large distance along a particular direction, then the TB method can be an efficient and accurate approach for electrostatic analysis for NEMS. In this paper, we present a coarse-grained tight binding approximation (CG-TBA) method, where the key idea is to represent the entire NEM structure with a minimal number of unit cells but to accurately compute the charge density and other electronic properties.

In the CG-TBA method if the electronic properties do not vary over a certain direction (e.g. the $z-$direction), then the unit cells along that direction are represented by just a single layer of unit cells. Similarly, if the charge density does not vary over a large distance along a particular direction (e.g. $x-$direction), then the unit cells used to define the large distance along that direction are again represented by a single layer of unit cells. In both these examples, the coarse-grained TBA reduces the full TB Hamiltonian into an equivalent reduced Hamiltonian i.e. mathematically the TB and the CG-TB formulations are equivalent. The CG-TBA can be implemented by a general algorithm to add simple modifications to the original Hamiltonian of a unit cell. In this paper, we also combine the CG-TBA method with the full TBA model to compute electronic properties on deformable nanostructures in an applied external field. The proposed method has several advantages: (1) coarse-graining significantly reduces the dimension of the full TBA Hamiltonian and the resulting eigensystem is much smaller; (2) The CG-TBA can be easily combined with original TBA. For a given NEM system, one can use full TBA and CG-TBA for different regions to compute the electronic properties accurately while avoiding unnecessary computational cost.

2 CG-TBA FOR SILICON LATTICE

The tight-binding method works by writing the eigenstates of the Hamiltonian matrix in an atomic-like basis set and replacing the exact many-body Hamiltonian operator with a parametrized Hamiltonian matrix. The eigenstates of the system are obtained self-consistently by solving the characteristic equation [4], [5]:

$$H\Psi_n = \epsilon_n \Psi_n \tag{1}$$

where $H = H_0 + \Delta H$ is the Hamiltonian, H_0 is the reference Hamiltonian corresponding to the material and the position of atoms, ΔH is the perturbed Hamiltonian due to an external field and the self-consistent redistribution of Mulliken charges, ϵ_n is the eigen energy and Ψ_n is the wavefunction. The matrix elements of the perturbed Hamiltonian ΔH are given by [5]

$$\Delta H_{ab}^{\alpha\beta} = \sum_{cd,\gamma\delta} U_{ab,cd}^{\alpha\beta,\gamma\delta} \left[\rho_{cd}^{\gamma\delta}(\epsilon_n, \Psi_n) - \rho_{cd}^{0\gamma\delta}(\epsilon_n^0, \Psi_n^0) \right] \tag{2}$$

where a, b, c and d denote the atoms, α, β, γ and δ denote the orbitals, the superscript 0 refers to the neutral unperturbed ground state, $\rho_{cd}^{\gamma\delta}$ is the density matrix and U is the two particle Coulomb integral. The TB parameters of silicon are chosen from [4]. Equations (1,2) are solved self-consistently to obtain the eigen energies and wavefunctions of the system.

2.1 Silicon Unit Cell TB Hamiltonian

Typically, silicon lattice is represented by unit cells. Without losing generality, a silicon structure placed in the Cartesian coordinate system is assumed to have NX, NY and NZ unit cells in the $x-$, $y-$ and $z-$direction, respectively. The atoms in a unit cell (i, j, k) are numbered as shown in Figure 1. Each atom belongs to a unit cell and each unit cell has 8 atoms. The total Hamiltonian H can be written as:

$$H = \{A\}_{(i,j,k)|(l,m,n)} \qquad (3)$$
$$i, l = 1, ..., NX;\ j, m = 1, ..., NY;\quad k, n = 1, ..., NZ$$

where $A_{(i,j,k)|(l,m,n)}$ is the Hamiltonian matrix representing the interaction between unit cells (i, j, k) and (l, m, n), and $\{A\}$ denotes an assembly of the A matrices. $A_{(i,j,k)|(l,m,n)}$ comprises 8×8 Hamiltonian submatrices representing the interaction between the atoms in the unit cells (i, j, k) and (l, m, n), i.e.,

$$A_{(i,j,k)|(l,m,n)}(a,b) = \begin{bmatrix} H_{ab}^{ss} & H_{ab}^{sp_x} & H_{ab}^{sp_y} & H_{ab}^{sp_z} \\ H_{ab}^{p_x s} & H_{ab}^{p_x p_x} & H_{ab}^{p_x p_y} & H_{ab}^{p_x p_z} \\ H_{ab}^{p_y s} & H_{ab}^{p_y p_x} & H_{ab}^{p_y p_y} & H_{ab}^{p_y p_z} \\ H_{ab}^{p_z s} & H_{ab}^{p_z p_x} & H_{ab}^{p_z p_y} & H_{ab}^{p_z p_z} \end{bmatrix} \qquad (4)$$

where $a, b = 1, 2, .., 8$, $a \in$ unit cell (i, j, k) and $b \in$ unit cell (l, m, n), and $H_{ab}^{\alpha\beta}$ is interaction energy between α orbital of atom a and β orbital of atom b, where $\alpha, \beta = s, p_x, p_y$ or p_z. Details of how to compute $H_{ab}^{\alpha\beta}$ can be found in [4]. Note that only the self-interactions and nearest neighbor interactions are considered in the TBA models. Therefore, the set of Hamiltonian matrices of non-zero interactions for an interior unit cell (i, j, k) can be rewritten as

$$\{A\}_{(i,j,k)|(l,m,n)} = \{A\}_{(i,j,k)|(i\pm 0/1, j\pm 0/1, k\pm 0/1)} \qquad (5)$$

Once the matrices $\{A\}_{(i,j,k)|(i\pm 0/1, j\pm 0/1, k\pm 0/1)}$ are obtained for all the unit cells in the system, the TB Hamiltonian in Eq. (3) can be assembled. Assuming the unit cells of the system are listed as $(1,1,1)$, ..., $(1,1,k)$, ..., $(1,1,NZ)$, $(1,2,1)$, ..., $(1,2,NZ)$, ..., $(1,j,k)$, ..., $(1,NY,NZ)$, ..., $(2,j,k)$, ..., (NX,NY,NZ), i.e., the index increases on k first, then on j and last on i. The TB matrix can be written in Eq. (6) (see next page).

2.2 Coarse-Grained TB Hamiltonian

In many applications of NEMS, the electronic properties does not vary over a large distance along a particular direction. In this case, the wavefunction remains

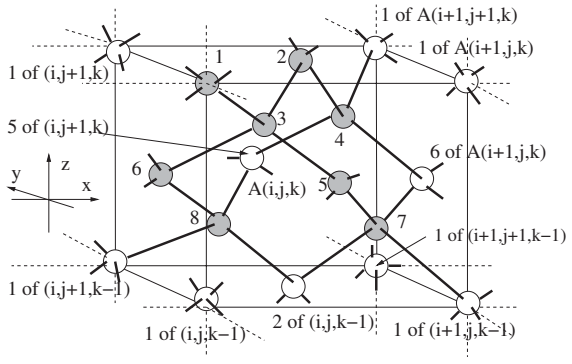

Figure 1: Atoms in the unit cell (i, j, k)

the same for the periodic unit cells over the large distance along that direction. Therefore, the unit cells used to define the large distance along that direction can be represented by a single layer of unit cells. This concept can be implemented by a reduction of the Hamiltonian matrix given in Eq. (6). For example, assuming the electronic properties have no variation in the $z-$direction, from Eq. (6), the rows in H corresponding to the unit cell $A_{(i,j,k)}$ can be written as

$$\begin{aligned} \overline{H}_{(i,j,k)} = \{&...A_{(i,j,k)|(i-1,j-1,k)}...A_{(i,j,k)|(i-1,j,k)} \\ &A_{(i,j,k)|(i-1,j,k+1)}...A_{(i,j,k)|(i,j-1,k)} \\ &A_{(i,j,k)|(i,j-1,k+1)}...A_{(i,j,k)|(i,j,k-1)}A_{(i,j,k)|(i,j,k)} \\ &A_{(i,j,k)|(i,j,k+1)}...A_{(i,j,k)|(i,j+1,k-1)} \\ &A_{(i,j,k)|(i,j+1,k)}...A_{(i,j,k)|(i+1,j,k-1)} \\ &A_{(i,j,k)|(i+1,j,k)}...A_{(i,j,k)|(i+1,j+1,k)}...\} \end{aligned} \qquad (7)$$

and the wavefunction vector is given by

$$\begin{aligned} \Psi_n^T = \{&...\Psi_{n(i-1,j-1,k)}...\Psi_{n(i-1,j,k)}\Psi_{n(i-1,j,k+1)}... \\ &\Psi_{n(i,j-1,k)}\Psi_{n(i,j-1,k+1)}...\Psi_{n(i,j,k-1)}\Psi_{n(i,j,k)} \\ &\Psi_{n(i,j,k+1)}...\Psi_{n(i,j+1,k-1)}\Psi_{(i,j+1,k)}...\Psi_{n(i+1,j,k-1)} \\ &\Psi_{n(i+1,j,k)}...\Psi_{n(i+1,j+1,k)}...\} \end{aligned} \qquad (8)$$

Note that all the nonzero elements for the unit cell (i, j, k) are listed in Eq. (7). Since the wavefunction does not vary over the periodic unit cells along $z-$direction, i.e.,

$$\Psi_{n(l,m,k-1)} = \Psi_{n(l,m,k)} = \Psi_{n(l,m,k+1)} \qquad (9)$$
$$l \in \{i, i \pm 1\}, m \in \{j, j \pm 1\},$$

substituting Eq. (9) into Eq. (8), Eq. (8) can be reduced and the elements that multiply the same wavefunction in Eq. (7) can be combinded. Equations (7,8) can be rewritten as

$$\begin{aligned} \overline{H}_{(i,j,k)} = \{&...A_{(i,j,k)|(i-1,j-1,k)}...(A_{(i,j,k)|(i-1,j,k)} \\ &+A_{(i,j,k)|(i-1,j,k+1)})...(A_{(i,j,k)|(i,j-1,k)} \\ &+A_{(i,j,k)|(i,j-1,k+1)})...(A_{(i,j,k)|(i,j,k-1)} \end{aligned}$$

$$H = \begin{bmatrix} A_{(1,1,1)|(1,1,1)} & \cdot & \cdot & \cdot & \cdot & \cdot & \cdot \\ \cdot & \cdot & \cdot & \cdot & \cdot & \cdot & \cdot \\ \cdot & \cdot & A_{(i,j,k-1)|(i,j,k-1)} & A_{(i,j,k-1)|(i,j,k)} & \cdot & \cdot & \cdot \\ \cdot & \cdot & A_{(i,j,k)|(i,j,k-1)} & A_{(i,j,k)|(i,j,k)} & A_{(i,j,k)|(i,j,k+1)} & \cdot & \cdot \\ \cdot & \cdot & \cdot & A_{(i,j,k+1)|(i,j,k)} & A_{(i,j,k+1)|(i,j,k+1)} & \cdot & \cdot \\ \cdot & \cdot & \cdot & \cdot & \cdot & \cdot & \cdot \\ \cdot & \cdot & \cdot & \cdot & \cdot & \cdot & A_{(NX,NY,NZ)|(NX,NY,NZ)} \end{bmatrix} \quad (6)$$

$$\begin{aligned} &+A_{(i,j,k)|(i,j,k)} + A_{(i,j,k)|(i,j,k+1)}) \\ &...(A_{(i,j,k)|(i,j+1,k-1)} + A_{(i,j,k)|(i,j+1,k)})... \\ &(A_{(i,j,k)|(i+1,j,k-1)} + A_{(i,j,k)|(i+1,j,k)})... \\ &A_{(i,j,k)|(i+1,j+1,k)}...\} \quad (10) \end{aligned}$$

$$\begin{aligned} \Psi_n^T = \{&...\Psi_{n(i-1,j-1,k)}...\Psi_{n(i-1,j,k)}...\Psi_{n(i,j-1,k)} \\ &...\Psi_{n(i,j,k)}...\Psi_{n(i,j+1,k)}...\Psi_{n(i+1,j,k)}... \\ &\Psi_{n(i+1,j+1,k)}...\} \quad (11) \end{aligned}$$

It is obvious that the k index for the Ψ vector in Eq. (11) can be omitted and by defining

$$A_{(i,j)|(l,m)} = \sum_{n=k-1}^{k+1} A_{(i,j,k)|(l,m,n)} \quad (12)$$
$$l \in \{i, i \pm 1\}, m \in \{j, j \pm 1\},$$

Eqs (10,11) can be rewritten further as

$$\begin{aligned} \overline{H}_{(i,j)} = \{&...A_{(i,j)|(i-1,j-1)}...A_{(i,j)|(i-1,j)}...A_{(i,j)|(i,j-1)} \\ &...A_{(i,j)|(i,j)}...A_{(i,j)|(i,j+1)}...A_{(i,j)|(i+1,j)}... \\ &A_{(i,j)|(i+1,j+1)}...\} \quad (13) \end{aligned}$$

$$\begin{aligned} \Psi_n^T = \{&...\Psi_{n(i-1,j-1)}...\Psi_{n(i-1,j)}...\Psi_{n(i,j-1)} \quad (14) \\ &...\Psi_{n(i,j)}...\Psi_{n(i,j+1)}...\Psi_{n(i+1,j)}...\Psi_{n(i+1,j+1)}...\} \end{aligned}$$

Therefore, the original TB equation, Eq. (1), can be reduced or coarse-grained to

$$\{A\}_{(i,j)|(l,m)}\Psi_{n(l,m)} = \epsilon_n \Psi_{n(i,j)} \quad (15)$$
$$i,l = 1,...,NX;\ j,m = 1,...,NY$$

Note that in Eq. (12), three layers of unit cells in the $z-$direction are needed to compute $\sum_{n=k-1}^{k+1} A_{(i,j,k)|(l,m,n)}$ for $n = k-1, k, k+1$. In this paper, we map the interactions between the atoms in different layers of unit cells to the interactions between the atoms in the unit cell (i,j,k). For example, considering $A_{(i,j,k)|(i,j,k-1)}$, the non-zero interactions are between atom 2 of unit cell $A_{(i,j,k-1)}$ and atoms 7,8 of unit cell $A_{(i,j,k)}$ as shown in Figure 1. It is easy to show mathematically that

$$A_{(i,j,k)|(i,j,k-1)}(7,2) = A_{(i,j,k)|(i,j,k)}(3,6) \quad (16)$$
$$A_{(i,j,k)|(i,j,k-1)}(8,2) = A_{(i,j,k)|(i,j,k)}(3,5) \quad (17)$$

Similarly, the other nonzero interactions in Eq. (12) can be computed by

$$A_{(i,j,k)|(i,j,k+1)}(2,7) = A_{(i,j,k)|(i,j,k)}(6,3) \quad (18)$$
$$A_{(i,j,k)|(i,j,k+1)}(2,8) = A_{(i,j,k)|(i,j,k)}(5,3) \quad (19)$$
$$A_{(i,j,k)|(i+1,j,k-1)}(7,1) = A_{(i,j,k)|(i,j,k)}(3,5) \quad (20)$$
$$A_{(i,j,k)|(i-1,j,k+1)}(1,7) = A_{(i,j,k)|(i,j,k)}(5,3) \quad (21)$$
$$A_{(i,j,k)|(i,j+1,k-1)}(8,1) = A_{(i,j,k)|(i,j,k)}(3,6) \quad (22)$$
$$A_{(i,j,k)|(i,j-1,k+1)}(1,8) = A_{(i,j,k)|(i,j,k)}(6,3) \quad (23)$$

Thus, the unit cells along the $z-$direction are coarse-grained to a single layer of unit cells (i,j) and Eq. (1) is reduced to Eq. (15). Coarse-grained TB Hamiltonian for the $x-$ and $y-$directions can be obtained in a similar manner.

3 RESULTS

In the first example, we compute the energy gap of a silicon nanofilm as shown in Figure 2. The thickness along the $z-$direction of the nanofilm, denoted as H_f in the figure, varies from 0.54nm to 11.95nm. Both the width and the length of the nanofilm are 17.4nm. In this case, the variation of the electronic properties in the nanofilm along the x-axis and the y-axis is negligible. We coarse-grain the nanofilm along both the $x-$ and $y-$directions, i.e., represent the entire nanofilm by a single column of unit cells in the $z-$direction. As shown in Figure 2, the energy gap as a function of film thickness calculated by using the CG-TBA method matches with the results obtained from the original TBA and the LDA methods [6].

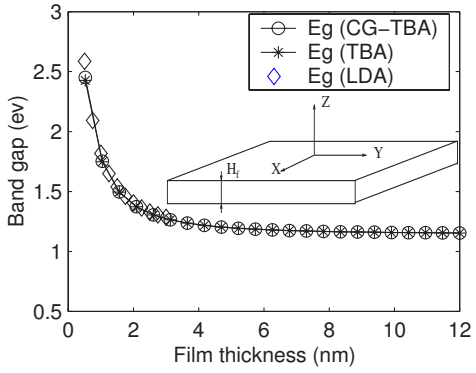

Figure 2: Energy gap variation of a silicon nanofilm

Figure 3 shows a nano capacitor with a N-doped(10^{17} cm^{-3}) silicon thin film located above an infinitely large ground plane and clamped at the ends with H = 2.6nm, L = 12.8nm, W = 40.2nm ($y-$axis is not shown). The 2nm gap is filled with silicon dioxide. It is clear that the variation of the charge density along the width direction ($y-$direction) is negligible. In this example, the unit cells in the $y-$direction are coarse-grained, i.e., all unit cells along the $y-$direction are replaced by a single layer of unit cells. Figure 3 shows the computed capacitance per unit length along the $y-$axis obtained from the original TBA method and the CG-TBA method. The two approaches give nearly identical results, while the computational cost is largely reduced by using the CG-TBA approach. As shown in Figure 4, for this example, the CPU time of the CG-TBA method is 10-30 times less than that of the original TBA method.

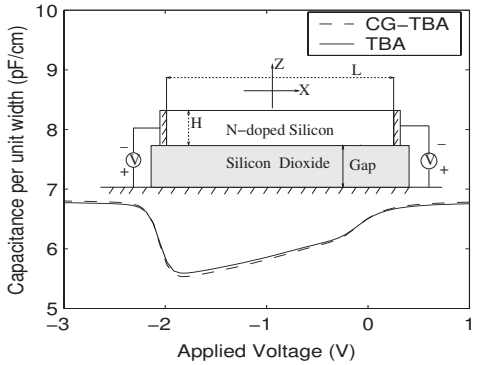

Figure 3: Capacitance of a silicon nanofilm as a function of applied voltage.

The third example, shown in Figure 5, is a silicon nanowire located above a ground plane and clamped at the ends with H = W = 2.6nm, L = 135.5nm, gap = 2nm and an applied voltage = 5V. Due to the large length of the nanowire, full TBA simulation of this device is very time consuming. Since the potential along the wire does not vary except near the ends, we employ the full TB model at the ends of the nanowire and coarse-grain the unit cells along the $x-$axis in the central part of the nanowire to a single layer of unit cells. The computed potential along the $x-$axis by combining CG-TBA with the full TBA is shown in Figure 5. In this example, by combining the CG-TBA and the full TBA, the CPU time for the analysis is reduced by about 100 times.

4 CONCLUSIONS

This paper presents a coarse-grained tight binding (CG-TBA) approach for electrostatic analysis of NEMS. In this approach, when the electronic properties do not vary over a large distance along a certain direction, the unit cells located within the distance along that direction are represented by just a single layer of unit cells. The approach significantly reduces the dimension of TB matrices and, consequently, the computational cost. Furthermore, the CG-TBA can be easily combined with the full TBA and one can use full TBA and CG-TBA for different regions in a nanostructure.

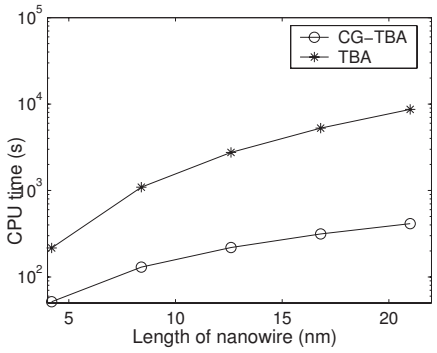

Figure 4: CPU time comparison of TBA and CG-TBA approaches.

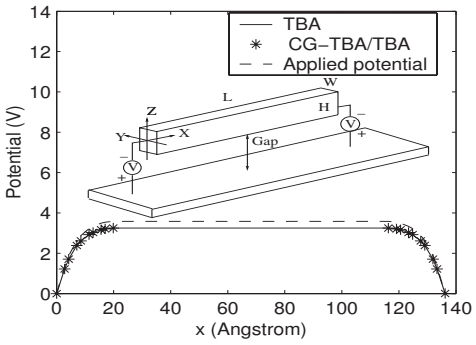

Figure 5: Potential profile of a nanowire in an external field.

ACKNOWLEDGMENTS

This work is partially supported by the Materials Computation Center at UIUC and the Network for Computational Nanotechnology.

REFERENCES

[1] M. L. Roukes,Solid State Sensor and Actuator Workshop, Hilton Head, 367, 2000.
[2] J.C.Slater et al, Phys. Rev., 94, 1498, 1954.
[3] W.A.Harrison, Phys. Rev. A, 7, 1876, 1973.
[4] J.A.Majewski et al, Phys. Rev. B, 35, 9666, 1987.
[5] K.Esfarjani et al, J. Phs.: Condens. Matter, 10, 8257, 1998.
[6] Y. M. Niquet et al, Phys. Rev. B, 62, 5109, 2000.